Journal of chemical & engineering data

Article

pubs.acs.org/jced

Design of a Gamma Densitometer for Hydrocarbon Fuel at High Temperature and Supercritical Pressure

Zhuqiang Yang, Qincheng Bi,* Yong Guo, Zhaohui Liu, Jianguo Yan, and Qiang Zhang

State Key Laboratory of Multiphase Flow in Power Engineering, Xi'an Jiaotong University, Xi'an, Shaanxi 710049, People's Republic of China

ABSTRACT: The densities of endothermic hydrocarbon fuel at supercritical pressure condition are measured online using a radial measurement method. The densitometer is based on the attenuation theory of gamma ray using a count rate mode. One advantage of the method is that it is noninstrusive and practical for a small tube measurement. The densitometer was measurably optimized for the design and calibrated by the reference fluids with different density ranges. A kind of endothermic hydrocarbon fuel was measured covering the temperature from (283 to 950) K at the supercritical pressures of (3.0 and 4.0) MPa. The data were regressed with polynomial equations and the isobaric thermal expansion could be obtained by the fitted density curve.

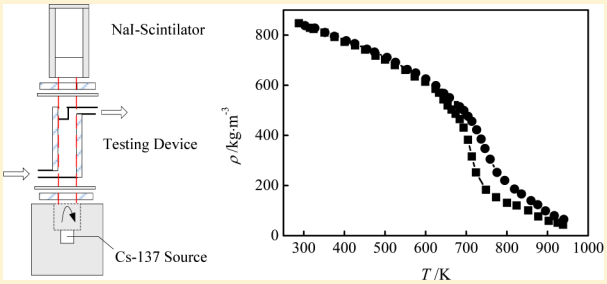

INTRODUCTION

Thermophysical properties of the fluid, such as specific heat, density, viscosity, surface tension, critical parameters, and so on, are the basis for calculation and the theoretical analysis of the experimental results. Knowledge of the density is also prerequisite for calculating other properties such as viscosity, thermal expansion, and flow regime, and so forth. As an important parameter, the density measurement is extremely demanded in the engineering application.

The densities of pure compounds[1−7] and binary[1,4,8−12] and ternary mixtures[13] have been investigated by many researchers who use piezometer devices,[9] vibrating tube densitometers,[10,13] or a rapid-heating sealed-ampule technique.[3−5] For the multicomponent hydrocarbon mixture, a measurement[14] based on the mass conservation equation was developed at sub- and supercritical conditions. Although the fore-mentioned densitometers are the popular methods for density measurement, the density data were studied at low temperature and different pressures. Meanwhile, their accuracies are closely influenced by the viscosity of fluids.

In some applications, the attenuation of radiation can serve as the basis for the density measurement. And the gamma densitometer has some advantages compared to the other methods. It is practical and reliable for obtain the density with a wide range of pressure. Most important, it is a nonintrusive technique that will never disturb the flow and eliminate the pressure drop and impact on the flow regime.

The radiation attenuation method for measuring density of a two-phase fluid was expounded in 1950s.[11] A "one-shot" and traverse method were compared for measuring the density and phase distribution. Afterward, a design procedure for a single-beam gamma densitometer and two densitometers was suggested for the flow boiling transient experiments.[7] The void fraction in gas−liquid flow in a small diameter tube was also measured using a gamma densitometer[12] and then optimized.[15−17] In a critical flow condition, research was devoted to the application of single-beam gamma densitometer in small diameter stainless steel pipe.[18] Some single-beam gamma densitometer measurements of oil−water flow were carried out in the horizontal and slightly inclined pipes.[8]

In the present work, a novel density measurement based on the gamma attenuation was conducted. The densities of an endothermic hydrocarbon fuel at supercritical pressure conditions were measured online within a large temperature range. The reliability and accuracy of the test measurement was verified strictly.

EXPERIMENTAL SECTION

Experimental System. The experiments were performed in the multiphase flow test facility in our laboratory. A schematic diagram of the experimental apparatus is shown in Figure 1.

The test fluids are driven by a constant flow pump (P270) with 100 mL/min supply capacity. A mass flow meter (MASS 2100 DI 1.5) is set up to real-time guarantee the specific flow to the measurement. A 40 μm and 7 μm filter is attached to the pump and the mass flow meter, respectively, to protect the devices from entrained impurity. The prepared fluid is electrically heated to a specific state by a high temperature alloy steel tube with length of 1500 mm. Finally, the fluid flowed into the test section.

In the test section, a pressure transducer (Rosemount 3051) is used to measure the work pressure controlled by a back

Received: April 8, 2014
Accepted: September 17, 2014
Published: October 1, 2014

   dx.doi.org/10.1021/je500314x | J. Chem. Eng. Data 2014, 59, 3335−3343

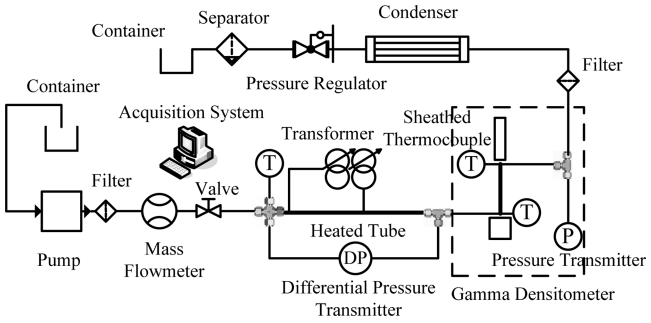

Figure 1. Schematic diagram of experimental system.

pressure valve at the outlet. The temperature is both measured at the inlet and outlet of the test pipe with two K-type armored thermocouples. The qualitative temperature in the experiments is defined by the average value of the two thermocouples. After testing, the hot fluid is cooled by a condenser and then flows through a separator into a container. All the useful information is recorded into a computer by a data acquisition system (IMP3595).

The detail configuration of the test section is shown in Figure 2. The gamma densitometer is equipped with a radioactive

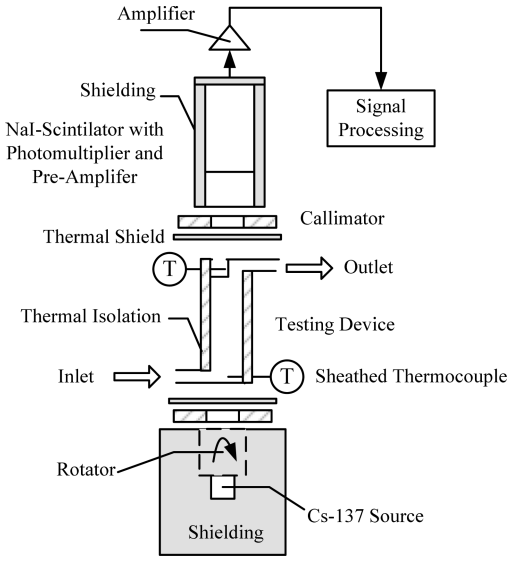

Figure 2. Detailed configuration of test section.

source, detector, and signal processing system. The radiation source and detector are sealed in a respective shielded container made of lead and located diametrically opposite along the pipe. The selection of each component of the densitometer depends on the geometry structure and flow characteristics of the test apparatus. In the experiments, the test pipe is made of stainless steel pipe with an inner diameter of 10.0 mm and length of 70.0 mm. Both of upper and lower coverplates are 2.0 mm in thickness equal to the wall ply.

The radioactive source should not only have monoenergetic gamma photons with high energy to penetrate the thick test section with measurable attenuation but also be low enough to be sensitive to the variation of the fluid content. The appropriate source should be chosen according to the designed situation, which is especially important in the present experiment. Considering the accuracy of the measurements, the cost, and the safety, the Cs-137 source was chosen, for it owes a medium energy and a high emission ratio. The strength of the source could be adjusted by a shielding rotator. When the switch is off, the source is entirely shielded from the environment.

As the detector of the gamma-ray, scintillator are demanded to have high detection efficiency and a short decay constant. They are necessary for avoiding "pileup" or saturation condition of the source operated in the count mode. Thus, NaI scintillator is used as the detector in the tests for its close to the 100 % detection efficiency and the relatively short decay time. In present design, the counting rate obtained is less than 10^4 counts s^{-1}, well below the maximum count rate (10^5 counts per second) where the detector becomes saturated.

The signal processing system would be chosen according to the count rates. The detector was connected to the photomultiplier tube and the gamma pulses were transformed to the photoelectrons and then to the electrodes voltages. The signal achieved from an amplifier was analyzed by a multichannel analyzer and counted by a counter. Finally, the signal was deal with by an exclusive processing program and saved into a computer.

To generate the narrow beam, the gamma-ray emission is supposed to be isotropic and well collimated. The circular slot with 10.0 mm diameter and 20.0 mm length are used as the source and detector collimator separately. There are two criterions on the selection on the size of the slot. One is to minimize the scattered photons contribution to the count rate, which is due to the Compton−Debye effect. The other is to maintain a large enough count rate to keep the small statistic error.

In the present study, both adiabatic and diabatic experiments were carried out. The thermal shield plates were located between the test pipe and the source (detector) to avoid the temperature influence on the source (detector). To decrease the heat loss of the test section, the ceramic tube with inside diameter of 14.0 mm wrapped the test pipe up.

Materials. The physical properties of test fluids are listed in Table 1. The hydrocarbon fuel l is made up of a blend of

Table 1. Sample Description

chemical name	source	initial mole fraction purity	purification method
water	own product	0.9995	pure deionized
nitrogen	Xi'an Yatai Air Co., Ltd.	0.998	none
cyclohexane	Aladdin Chemistry	0.995	distillation
n-heptane	Aladdin Chemistry	0.995	distillation
n-octane	Aladdin Chemistry	0.995	distillation
fuel	Karamay Oil		distillation

hydrocarbons, with w = 0.8140 cycloalkanes, w = 0.0475 alkanes, w = 0.0488 alkenes, w = 0.0400 aromatics, and w = 0.0497 others. The fuel's critical pressure and temperature are measured to be about 2.35 MPa and 694.1 K due to the critical opalescence phenomenon. The detailed compositions of the hydrocarbon fuel analyzed by Agilent GC6890-MS5973 are listed in Table 2.

Theory. The gamma-ray attenuation of the densitometer is based on the fact that the electromagnetic radiation is attenuated when it passes through matter owing to the interaction of its photons. In this work, the gamma densitometer concerned the photoelectric interactions and the Compton scattering interactions should be minimized. The

dx.doi.org/10.1021/je500314x | J. Chem. Eng. Data 2014, 59, 3335−3343

Table 2. Detailed Compositions of Hydrocarbon Fuel

fuel number	composition	mass fraction
1	decahydronaphthalene	0.0181
2	2-methyl-bicyclo[2.2.2]octane	0.0290
3	5-undecene	0.0133
4	2-methyl-trans-decalin	0.1621
5	2-syn-methyl-cis-decalin	0.0870
6	decahydro-2,6-dimethyl-naphthalene	0.1291
7	1,2,3,4-tetrahydro-1,4-dimethyl-naphthalene	0.0123
8	trans,cis-1,8-Dimethylspiro[4.5]decane	0.0551
9	7-pentyl-bicyclo[4.1.0]heptane	0.0162
10	1-(1-methylethenyl)-2-(1-methylethyl)-benzene	0.0290
11	4-(2-butenyl)-1,2-dimethyl-(*E*)-benzene,	0.0039
12	1-methyl-4-(1-methylbutyl)-cyclohexane	0.0225
13	2-butyl-1,1,3-trimethyl-cyclohexane	0.0493
14	2,6-dimethyl-undecane,	0.0450
15	cis,trans-1,9-Dimethylspiro[5.5]undecane	0.0444
16	3-methyl-7-pentyl-bicyclo[4.1.0]heptane	0.0943
17	2-methyl-7-pentyl-bicyclo[4.1.0]heptane	0.0590
18	2-hexyl-bicyclo[2.2.1]heptane	0.0291
19	1-nonadecene	0.0052
20	7-methyl-6-tridecene	0.0303
21	others	0.0658

intensity of a gamma beam decreases exponentially and is governed by the Beer−Lambert's law

$$I = I_0\exp[-(\mu/\rho)\cdot\rho x] \tag{1}$$

where I_0 is the incident radiation intensity and I is the intensity of detected radiation through the absorption materials with a distance x. ρ represents the density of the absorption material and stands for the average density of the fluid in a certain volume in our experiments. The capability of material to absorb γ radiation is characterized by its mass absorption coefficient μ/ρ. It depends on the chemical composition of the material and the energy of the γ rays. In other words, the mass absorption coefficient would not vary when the chemical composition of the material and radiation energy remain the same.

When the test pipe is filled with the fluid at specific state, the attenuation of the γ radiation can be given as

$$I = I_0\exp[-(\mu/\rho)_f\rho_f x]\cdot[-(\mu/\rho)_w\rho_w x_w] \tag{2}$$

where w and f stand for the wall of the test pipe and fluid in the pipe, respectively.

Similarly, the intensity of a high density fluid filled test volume is given as

$$I_H = I_0\exp[-(\mu/\rho)_H\rho_H x]\cdot[-(\mu/\rho)_w\rho_w x_w] \tag{3}$$

The analogous intensity of a low density fluid filled test volume can be expressed as

$$I_L = I_0\exp[-(\mu/\rho)_L\rho_L x]\cdot[-(\mu/\rho)_w\rho_w x_w] \tag{4}$$

Equations 2 to 4 can be combined to obtain a logarithmic relation given as

$$\ln\left(\frac{I_H}{I_L}\right) = (-\mu/\rho)_H\rho_H x - (-\mu/\rho)_L\rho_L x \tag{5}$$

$$\ln\left(\frac{I_H}{I}\right) = (-\mu/\rho)_H\rho_H x - (-\mu/\rho)_f\rho_f x \tag{6}$$

Then the above two formulas are combined to a relation as follows:

$$\ln\left(\frac{I_H}{I_L}\right)/\ln\left(\frac{I_H}{I}\right) = \frac{(-\mu/\rho)_H\rho_H - (-\mu/\rho)_L\rho_L}{(-\mu/\rho)_H\rho_H - (-\mu/\rho)_f\rho_f} \tag{7}$$

When the values of the mass absorption coefficient of three fluids are almost the same, then eq 7 can be transformed as

$$\rho = \rho_H + (\rho_L - \rho_H)\cdot\frac{\ln(I/I_H)}{\ln(I_L/I_H)} \tag{8}$$

If the mass absorption coefficient of the low density fluid is far less than others, then eq 7 can be converted as

$$\rho = \rho_H - \rho_H\cdot\frac{\ln(I/I_H)}{\ln(I_L/I_H)} \tag{9}$$

As the count rate of the densitometer was proportion to the intensity of the radiations detected for a certain area, the final format of the theory formula can be expressed as

$$\rho = \rho_H + (\rho_L - \rho_H)\cdot\frac{\ln(\Phi/\Phi_H)}{\ln(\Phi_L/\Phi_H)} \tag{10}$$

$$\rho = \rho_H - \rho_H\cdot\frac{\ln(\Phi/\Phi_H)}{\ln(\Phi_L/\Phi_H)} = \rho_H\frac{\ln(\Phi_L/\Phi)}{\ln(\Phi_L/\Phi_H)} \tag{11}$$

where Φ is the count rate of the densitometer, so Φ_H and Φ_L stand for the count rate of the high and low density fluid, respectively. The density of the test fluid can be obtained by the measured count rate of the fluid and two reference data with different densities, whose range consists of the test density.

A high test fluid transmission ratio must be required to design an appropriate densitometer system. The small statistical error of the count measurement for the gamma densitometer in the count mode is the most important parameter in the whole process. The statistical error is inversely proportional to the sensitivity and the square root of the count number as follows:

$$\varepsilon = \frac{1}{S\sqrt{N}} \tag{12}$$

Here, N is the number of photons detected by the signal system during the certain count time and S is the sensitivity of the gamma beam to the test content in the test pipe

$$S = \frac{N_1 - N_0}{(N_1 - N_0)/2} \tag{13}$$

According to eq 11, the combined standard uncertainty of measured density $u_c(\rho)$ is

$$u_c^2(\rho) = \left(\frac{\partial\rho}{\partial\rho_H}\right)^2 u^2(\rho_H) + \left(\frac{\partial\rho}{\partial\Phi_L/\Phi}\right)^2 u^2(\Phi_L/\Phi) + \left(\frac{\partial\rho}{\partial\Phi_L/\Phi_H}\right)^2 u^2(\Phi_L/\Phi_H) \tag{14}$$

In this work, the statistical uncertainty of the count number is (0.683 to 3.416), so the relative standard uncertainty of the Φ_H, Φ_L, and Φ have been identified as (0.0329 to 0.165) %, (0.0490 to 0.246) %, and (0.0333 to 0.246) %. The relative standard uncertainty of (Φ_L/Φ), (Φ_L/Φ_H), and ρ_H are calculated as (0.0592 to 0.348) %, (0.0590 to 0.296) %, and (0.100 to 1.458) %, respectively. Thus, the combined standard

dx.doi.org/10.1021/je500314x | J. Chem. Eng. Data 2014, 59, 3335−3343

uncertainty of density is calculated as (0.146 to 1.143) %. The relative expanded uncertainty of density measurement is identified as (0.292 to 2.286) % (coverage factor k = 2).

RESULTS AND DISCUSSION

Calibration of the Gamma-Densitometer. The gamma-densitometer is a radiation detection system. It is necessary to deal with several factors and parameters, which would affect the relation between the radiation source emission and the response of the detector, that is, the count rate. These parameters include the distance between the source and detector, time dependency of the system, the length of the test pipe, the slot size of the collimator, and the influence of the temperature.

Distance between the Source and Detector. Several tests were conducted to investigate the influence of the distance between the source and the detector. The results are shown in Figure 3, in which the distance between the source and the upper end of the test pipe varied 3.0 mm to 10.0 mm and the distance between the detector and lower end varied between 5.0 mm and 60.0 mm. As a result, the difference of count rate according to the test pipe filled with water and gas becomes largest when the distance is 3.0 mm upstream and 5.0 mm downstream. That is to say that the source and detector should close enough to the test pipe in the experiments.

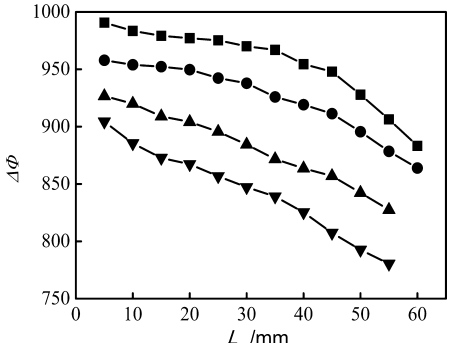

Figure 3. Influence of the distance between test pipe and source L_s (detector L_d) on the count rate. ■, L_s = 3.0 mm; ●, L_s = 5.0 mm; ▲, L_s = 8.0 mm;▼, L_s = 10.0 mm.

Time Dependency of the System and the Temperature Influence. Figure 4 shows the measuring time against the count rate and the cumulative sum of the count. It is clear that the correlation between the count and the time is perfect linear and the count rate is almost the constant during the measuring period of the experiments (around 540 s). It says the measurement for the count rate in the specific device is credible.

In addition, the dependence of the count rate on the ambient and test pipe temperature was examined. The temperature of the tube varied from room temperature to high temperature. As shown in Figure 5, the count rate is nearly constant with the variation of the temperature. That indicates a weak dependency on the temperature due to the well protection of the thermal shielding and heat isolation on the test pipe.

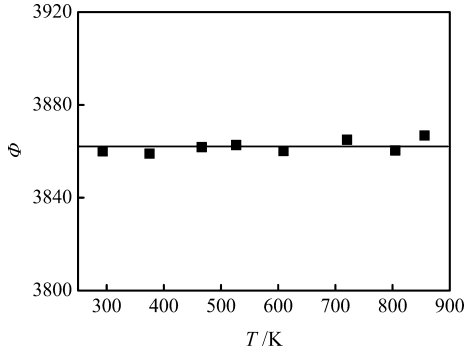

Figure 5. Dependence of the count rate on the temperature.

Influence of the Length of the Test Pipe and the Slot Size. To ensure the accuracy of measured density, the count rate is supposed to be large enough. Meanwhile the sensitivity calculated by eq 13 requires a small count rate. According to the two criterions, the length of the test pipe was chosen with seven times to pipe diameter. With the longer length of the test pipe, the ratio of the attenuated ray occupied by the test fluid becomes large, which will improve the sensitivity of the densitometer.

The slot of collimators with the same size with tube diameter was adopted in the experiments. The larger size of the slot may increase the counting error caused by the scattered photons, but the smaller size could not express the real content on the whole pipe section.

Calibration of the Reference Substances. For an accurate test, the measuring instruments are necessary to calibrate with suitable reference standards. The pressure transducer was calibrated by float type manometer (Y055). And the calibration of the thermocouples was conducted using JOFRA temperature calibrator (650SE). The uncertainties were 0.0075 MPa for pressure and 1.75 K for temperature. The mass

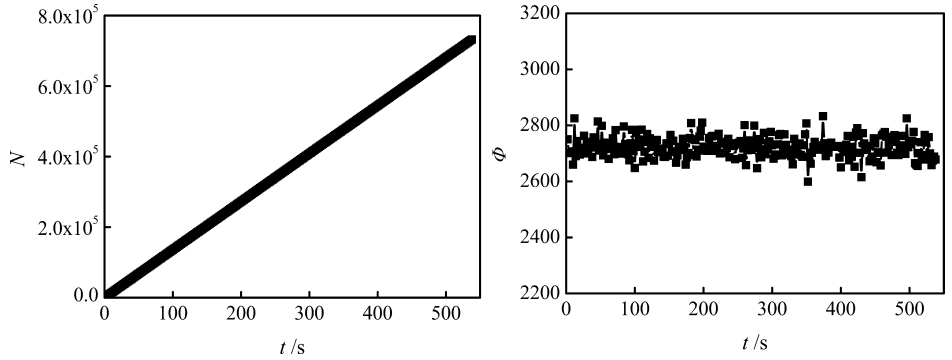

Figure 4. Time dependency of the count rate in the system.

dx.doi.org/10.1021/je500314x | J. Chem. Eng. Data 2014, 59, 3335−3343

Table 3. Experimental Values and Reference Data of Density ρ at Temperature T, Pressure p, and Relative Differences $\Delta\rho/\rho = (\rho_{exp} - \rho_{ref})/\rho_{ref}$ for the Water[a]

T	ρ_{exp}	ρ_{ref}	$\Delta\rho/\rho$	T	ρ_{exp}	ρ_{ref}	$\Delta\rho/\rho$
K	kg·m^{-3}	kg·m^{-3}	%	K	kg·m^{-3}	kg·m^{-3}	%
	p = 5.0 MPa				p = 3.0 MPa		
288.3	1001.4	1001.4	0.00	286.0	1000.7	1000.8	−0.01
303.5	996.5	997.7	−0.12	305.0	996.2	996.4	−0.02
324.8	990.7	989.4	0.13	322.6	988.4	989.6	−0.12
344.3	981.8	979.3	0.26	343.4	977.7	978.9	−0.13
358.6	966.8	970.5	−0.38	356.4	969.0	971.0	−0.20
372.3	957.1	961.2	−0.43	374.7	962.3	958.6	0.39
384.0	947.0	952.7	−0.60	391.2	945.0	946.0	−0.11
393.6	938.5	945.2	−0.70	412.5	927.7	928.1	−0.04
403.8	932.6	936.8	−0.44	423.8	920.4	917.8	0.28
414.2	923.0	927.7	−0.50	442.5	899.6	899.6	0.00
423.2	915.2	919.5	−0.47	462.5	880.9	878.1	0.32
432.8	903.3	910.4	−0.77	471.4	873.1	867.8	0.61
442.7	893.8	900.5	−0.75	483.9	858.3	852.6	0.67
452.6	884.3	890.2	−0.66	492.5	841.7	841.7	0.00
462.0	876.7	880.1	−0.38	500.4	827.9	831.1	−0.38
474.3	864.5	866.0	−0.17				
484.1	854.6	854.1	0.06				
491.4	839.5	844.9	−0.64				
502.5	824.9	830.2	−0.63				
511.0	814.1	818.2	−0.50				

[a]Standard uncertainties u are $u(T)$ = 1.75 K, $u(p)$ = 0.004 MPa and the combined expanded uncertainty U_c is $U_c(\rho)$ = 2.8 kg·m^{-3} (0.95 level of confidence).

flow meter was calibrated by weighing the flow over a period of time at a constant flow rate and the accuracy is 0.01 g.

The gamma densitometer should be calibrated by a well-known substance for the hydrocarbon fuel measurement. For the purpose, nitrogen, water, and cyclohexane were chosen as the reference pure substance. The binary mixture of w = 0.500 n-heptane and w = 0.500 n-octane were also tested. Densities for the reference fluids measured in experiments were compared with the data available at NIST. In the calculation, the percentage deviation (PD), the average absolute deviation (AAD), and the maximum absolute deviation (MAD) of the results are set as

$$\mathrm{PD} = \left(\frac{\rho_{\mathrm{measured}}}{\rho_{\mathrm{referenced}}} - 1\right) \times 100\% \tag{15}$$

$$\mathrm{AAD} = \frac{\sum_{i=1}^{n} \mathrm{abs}(PD_i)}{n} \tag{16}$$

$$\mathrm{MAD} = \max(\mathrm{abs}(PD_i)) \tag{17}$$

Experimental densities of water were measured at constant pressure (p = 3.0 MPa and 5.0 MPa) with a wide temperature range under the compressed liquid state. Good agreement was achieved in Table 3 and Figure 6. The MAD was within the 1 % and the AAD was just 0.43 % at p = 5.0 MPa. When the pressure was 3.0 MPa, The MAD was also within the 1 % and the AAD was limited to 0.22 %. Taking into account the experimental uncertainty, the reliability of the densitometer for the compressed liquid was confirmed.

Nitrogen used as reference fluid was tested at constant temperature and pressure from 0.1 MPa to 6.0 MPa. The densities of the nitrogen were obtained at T = 293.2 K and 473.2 K as shown in Figure 7 and Table 4. As the compressed

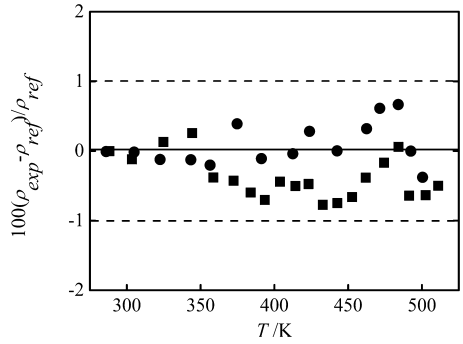

Figure 6. Deviation of measured and referenced densities of water versus temperature. ■, p = 5.0 MPa; ●, p = 3.0 MPa.

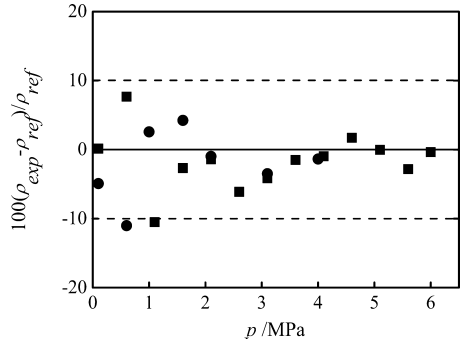

Figure 7. Deviation of measured and referenced densities of nitrogen versus pressure. ■, T = 293.2 K; ●, T = 473.2 K.

gas, the variation of the nitrogen was not easy to be identified especially in the low pressure. It can be seen that the MAD was about 10 % at several bar pressure. And with the pressure increase, the deviation became smaller. The AAD was

dx.doi.org/10.1021/je500314x | J. Chem. Eng. Data 2014, 59, 3335−3343

Table 4. Experimental Values and Reference Data of Density ρ at Temperature T, Pressure p and Relative Differences $\Delta\rho/\rho = (\rho_{exp} - \rho_{ref})/\rho_{ref}$ for the Nitrogen[a]

p	ρ_{exp}	ρ_{ref}	$\Delta\rho/\rho$	p	ρ_{exp}	ρ_{ref}	$\Delta\rho/\rho$
MPa	kg·m^{-3}	kg·m^{-3}	%	MPa	kg·m^{-3}	kg·m^{-3}	%
	T = 293.2 K				T = 473.2 K		
6.0	69.11	69.36	−0.36	4.0	27.65	28.03	−1.36
5.6	62.20	64.00	−2.82	3.1	21.05	21.81	−3.48
5.1	58.28	58.30	−0.03	2.1	14.69	14.83	−0.98
4.6	53.49	52.59	1.71	1.6	11.8	11.32	4.24
4.1	46.43	46.87	−0.95	1.0	8.00	7.80	2.58
3.6	40.54	41.15	−1.49	0.6	3.79	4.26	−11.01
3.1	33.96	35.42	−4.15	0.1	0.68	0.71	−4.92
2.6	27.88	29.70	−6.11				
2.1	23.64	23.98	−1.40				
1.6	17.77	18.25	−2.67				
1.1	11.22	12.54	−10.51				
0.6	7.36	6.83	7.68				
0.1	1.150	1.151	0.15				

[a]Standard uncertainties u are $u(T)$ = 1.75 K, $u(p)$ = 0.004 MPa and the combined expanded uncertainty U_c is $U_c(\rho)$ = 0.8 kg·m^{-3} (0.95 level of confidence).

respective 3.08 % and 4.41% at T = 293.2 K and 473.2 K. All the results show that the density of the compressed gas could be well measured with this test method.

As the pure substance, the densities of cyclohexane were measured at constant supercritical pressure 5.0 MPa with temperature from 283 K to 698 K as shown in Figure 8 and

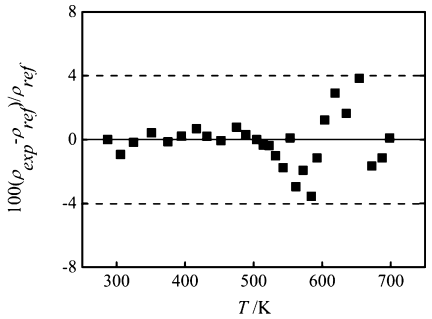

Figure 8. Deviations of measured and referenced densities of cyclohexane versus temperature at p = 5.0 MPa.

Table 5. The changing process of the density would undergo the compressed liquid and supercritical fluid state. Thus, there was a huge change of density with the temperature increases. The results show a fine agreement with the reference data, where the MAD was limited to 4 % and the AAD was 0.80 % in the whole range.

The densities of w = 0.500 n-heptane and w = 0.500 n-octane mixture were measured at constant pressure 5.1 MPa with temperature from 303 K to 591 K. The results were illustrated in Figure 9 and Table 6, compared with the values available at NIST. It shows that the MAD was limited to 1.54 % and the AAD was 0.38 %. Moreover, different mass ratio binary mixture of n-heptane and n-octane were performed and compared with density measurement reported in literature[9] as shown in Table 7. This excellent agreement further confirms the reliability and accuracy of the present measurements for mixtures.

All the three sets of tests were performed to provide validation and accuracy for our density measurement. As

Table 5. Experimental Values and Reference Data of Density ρ at Temperature T, Pressure p, and Relative Differences $\Delta\rho/\rho = (\rho_{exp} - \rho_{ref})/\rho_{ref}$ for Cyclohexane[a]

T	ρ_{exp}	ρ_{ref}	$\Delta\rho/\rho$	T	ρ_{exp}	ρ_{ref}	$\Delta\rho/\rho$
K	kg·m^{-3}	kg·m^{-3}	%	K	kg·m^{-3}	kg·m^{-3}	%
			p = 5.0 MPa				
287.0	788.3	788.3	0.00	543.0	454.5	462.7	−1.76
305.9	763.7	771.0	−0.94	553.2	426.2	425.8	0.10
324.9	752.1	753.4	−0.18	561.7	365.6	376.7	−2.96
351.0	731.8	728.7	0.42	572.1	259.5	264.6	−1.93
375.0	704.3	705.2	−0.14	584.2	187.0	193.9	−3.56
394.8	686.7	685.2	0.22	592.5	167.0	169.0	−1.15
416.6	666.5	662.0	0.68	603.6	149.3	147.5	1.22
431.9	646.2	644.9	0.20	618.8	133.0	129.2	2.91
452.4	620.2	620.6	−0.07	635.0	118.3	116.4	1.64
475.1	595.5	590.9	0.77	654.2	109.8	105.7	3.84
488.4	573.5	571.7	0.32	672.3	96.5	98.2	−1.66
504.4	546.3	546.3	−0.00	687.5	92.0	93.0	−1.15
513.9	527.5	529.4	−0.35	698.5	89.9	89.8	0.10
522.6	510.3	512.3	−0.38				
531.9	487.0	492.0	−1.02				

[a]Standard uncertainties u are $u(T)$ = 1.75 K, $u(p)$ = 0.004 MPa and the combined expanded uncertainty U_c is $U_c(\rho)$ = 2.2 kg·m^{-3} (0.95 level of confidence).

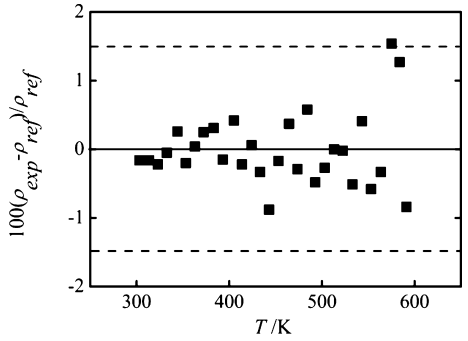

Figure 9. Deviations of measured and referenced densities of w = 0.500 n-heptane and w = 0.500 n-octane mixture versus temperature at p = 5.1 MPa.

application promotion, the densities of the hydrocarbon fuel were measured. In the supercritical pressure condition, the fuels versus temperature will undergo the compressed liquid, the supercritical fluid and the compressed gas states.[19]The densities of the hydrocarbon fuel have been measured with a temperature range of (283 to 950) K at supercritical pressure 3.0 and 4.0 MPa. The data are shown in Table 8.

Figure 10 presents the density variations of the fuel under operation condition. The density decreases as temperature increases gradually. And the density decreases dramatically when the temperature reaches to above 710 K for 3.0 MPa fuel and 730 K for 4.0 MPa. The kickpoints are accordant with the measured temperature on the critical special phenomenon. As temperature further increases, the trend of the variation of the fuel density becomes smooth. From the density curves, some parameters of the flow and heat transfer characteristics could be obtained.

Isobaric Thermal Expansion of the Hydrocarbon Fuel. The isobaric thermal expansion can be obtained by the measured density. It is defined as

dx.doi.org/10.1021/je500314x | J. Chem. Eng. Data 2014, 59, 3335−3343

Table 6. Experimental Values and Reference Data of Density ρ at Temperature T, Pressure p, and Relative Differences $\Delta\rho/\rho = (\rho_{exp} - \rho_{ref})/\rho_{ref}$ for the w = 0.500 *n*-Heptane and w = 0.500 *n*-Octane Mixture[a]

T	ρ_{exp}	ρ_{ref}	$\Delta\rho/\rho$	T	ρ_{exp}	ρ_{ref}	$\Delta\rho/\rho$
K	kg·m^{-3}	kg·m^{-3}	%	K	kg·m^{-3}	kg·m^{-3}	%
			p = 5.1 MPa				
303.1	686.2	687.3	−0.16	453.1	554.4	555.3	−0.17
313.3	678.1	679.2	−0.16	464.5	545.2	543.2	0.37
323.0	670.0	671.4	−0.22	473.6	531.6	533.1	−0.29
332.7	663.3	663.6	−0.05	484.2	524.0	520.9	0.58
344.1	655.9	654.2	0.26	492.8	508.0	510.4	−0.48
353.2	645.5	646.8	−0.20	503.1	495.9	497.3	−0.27
362.9	638.9	638.6	0.04	513.2	483.6	483.6	0.00
372.3	632.3	630.7	0.25	522.4	470.1	470.2	−0.02
383.2	623.2	621.3	0.31	533.0	451.2	453.5	−0.51
393.0	611.8	612.7	−0.15	543.3	437.7	435.9	0.41
405.1	604.3	601.8	0.42	553.0	415.1	417.6	−0.58
413.8	592.5	593.8	−0.22	563.5	394.0	395.3	−0.33
424.2	584.4	584.1	0.06	575.1	372.9	367.3	1.54
433.2	573.5	575.4	−0.33	583.8	348.2	343.8	1.27
443.0	560.6	565.6	−0.88	591.2	319.0	321.7	−0.84

[a]Standard uncertainties u are $u(T)$ = 1.75 K, $u(p)$ = 0.004 MPa and the combined expanded uncertainty U_c is $U_c(\rho)$ = 2.1 kg·m^{-3} (0.95 level of confidence).

Table 7. Experimental Values and Reference Data of Density ρ at Temperature T, Pressure p, and Relative Differences $\Delta\rho/\rho = (\rho_{exp} - \rho_{ref})/\rho_{ref}$ for the *n*-Heptane and *n*-Octane Mixture[a]

p	T	ρ_{exp}	p	T	ρ_{ref}	$\Delta\rho/\rho$
MPa	K	kg·m^{-3}	MPa	K	kg·m^{-3}	%
			w = 0.255 *n*-Heptane and w = 0.745 *n*-Octane			
	This work			Abdulagatov et. al[9]		
3.3	374.7	633.2	3.256	374.79	634.7	−0.24
8.0	374.8	640.4	8.081	374.79	641.5	−0.17
3.5	429.4	584.0	3.511	429.34	585.6	−0.27
8.3	429.4	592.3	8.237	429.34	595.9	−0.61
4.4	475.8	538.4	4.354	475.85	539.5	−0.21
8.5	475.9	554.4	8.492	475.85	553.8	0.11
4.7	525.5	473.6	4.771	525.5	475.8	−0.46
7.3	525.5	493.5	7.331	525.5	494.9	−0.28
5.3	557.2	427.1	5.296	557.23	430.4	−0.77
8.2	557.2	460.9	8.238	557.23	461.5	−0.13
			w = 0.510 *n*-Heptane and w = 0.490 *n*-Octane			
	This work			Abdulagatov et. al[9]		
3.2	380.5	619.9	3.11	380.43	623.5	−0.58
8.7	380.5	631.1	8.743	380.43	633.1	−0.32
4.9	424.4	582.4	4.903	424.48	588.7	−1.07
7.2	424.5	588.0	7.108	424.48	592.8	−0.81
3.2	466.6	535.5	3.177	466.78	538.3	−0.52
8.6	466.7	554.2	8.649	466.78	556.8	−0.47
4.9	518.0	479.1	4.982	518.04	480.1	−0.21
7.5	518.0	494.8	7.512	518.04	496.2	−0.28
5.4	549.3	427.9	5.394	549.34	431.7	−0.88
8.7	549.4	461.2	8.689	549.34	464.6	−0.73

[a]Standard uncertainties u are $u(T)$ = 1.75 K, $u(p)$ = 0.004 MPa and the combined expanded uncertainty U_c is $U_c(\rho)$ = 2.1 kg·m^{-3} (0.95 level of confidence).

Table 8. Experimental Values of Density ρ at Temperature T and Pressure p for the Fuel at Supercritical Pressure Conditions[a]

T	ρ	T	ρ	T	ρ	T	ρ
K	kg·m^{-3}	K	kg·m^{-3}	K	kg·m^{-3}	K	kg·m^{-3}
			p = 3.0 MPa				
288.0	847.3	500.1	702.1	663.8	503.0	800.3	131.1
315.2	828.9	524.2	680.0	673.7	486.1	823.9	120.4
324.2	824.4	550.1	661.0	683.9	464.9	852.5	100.9
351.0	810.1	573.1	634.8	693.4	430.8	877.2	76.6
375.6	792.5	599.1	613.9	704.2	382.6	903.0	59.2
400.4	769.0	624.3	585.5	713.7	315.9	924.8	51.6
426.3	759.0	633.0	570.2	723.9	252.4	938.2	43.8
451.0	742.0	643.7	543.3	748.4	183.2		
476.6	717.6	654.1	519.3	773.4	153.3		
			p = 4.0 MPa				
303.0	837.6	525.9	691.5	694.1	499.3	818.7	186.0
327.2	828.1	554.7	663.0	704.5	475.9	835.8	166.3
352.0	810.5	575.6	649.0	713.8	456.1	859.3	139.9
375.4	795.2	600.3	625.3	725.5	422.4	876.0	123.5
404.5	777.6	625.1	598.5	736.6	385.4	894.9	99. 1
425.5	766.2	644.8	567.6	746.0	347.6	916.6	80.0
455.4	743.8	658.7	550.4	758.8	305.1	941.2	65.3
474.2	732.4	675.6	527.3	775.6	252.2		
504.8	711.1	683.7	514.5	794.6	220.4		

[a]Standard uncertainties u are $u(T)$ = 1.75 K, $u(p)$ = 0.004 MPa and the combined expanded uncertainty U_c is $U_c(\rho)$ = 2.3 kg·m^{-3} (0.95 level of confidence).

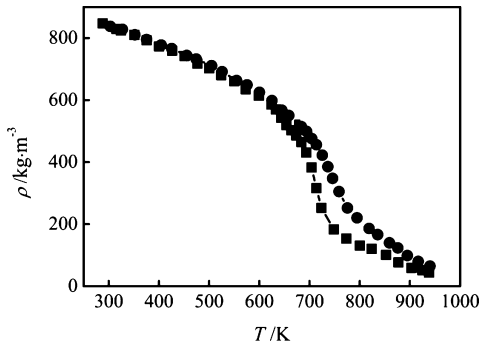

Figure 10. Density variations of hydrocarbon fuel versus temperature at: ■, p = 3.0 MPa.; ●, p = 4.0 MPa.

$$\alpha_p = -\frac{1}{\rho}\left(\frac{\partial\rho}{\partial T}\right)_p \quad (18)$$

Figure 11 shows the results of the isobaric thermal expansion of the fuels versus temperature at supercritical pressures. It is found that α_p varies nonmonotony with the temperature increasing. It reaches the first peak value around its pseudocritical temperature with the increase of the temperature due to the largest variation of the thermophysical properties. The temperature corresponding to the peak value differs with pressures and the peak value usually varies. With the temperature further increases, the value of the thermal expansion would be enhanced again due to the chemical endothermic reactions and the increased gas generation rate. However, the polyreaction and the existence of gas layer beside the tube wall would decrease the thermal expansion values in high temperature. The variation of α_p at supercritical pressure is complex and closely related to the experimental phenomenon.

dx.doi.org/10.1021/je500314x | J. Chem. Eng. Data 2014, 59, 3335−3343

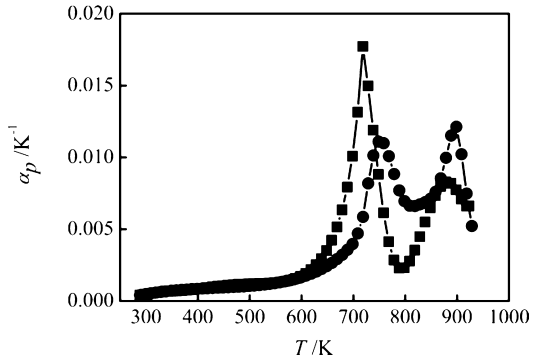

Figure 11. Effect of temperature on the isobaric thermal expansion: ■, p = 3.0 MPa; ●, p = 4.0 MPa.

■ CONCLUSION

A novel density measurement method is proposed based on the attenuation theory of gamma ray through the materials for the single phase and supercritical fluids within a large temperature extent. A comprehensive set of experimental tests were conducted to examine the densitometer and optimize the instrumentation. The accuracy of the densitometer was calibrated by reference fluids with different density range. Water was measured at the pressure of 5.0 and 3.0 MPa in a compressed liquid state. The measured average absolute deviation (AAD) is 0.43 % and 0.22 %, and the maximum absolute deviation (MAD) is within 1 %, respectively. The densities of the nitrogen were obtained at specific temperatures in a compressed gas state. The measured average absolute deviation (AAD) is 4.20 % and 5.09 % at 293.2 K and 473.2 K, respectively, and the maximum absolute deviation (MAD) is about 10 % at several bar pressure. The densities of cyclohexane were measured at supercritical pressure 5.0 MPa with temperature from 283 K to 698 K. The measured average absolute deviation (AAD) was 0.80 % and the maximum absolute deviation (MAD) was limited to the 4 %. As a binary mixture, densities of w = 0.500 n-heptane and w = 0.500 n-octane mixture were measured at constant pressure 5.1 MPa with temperature from 303 K to 591 K. The maximum absolute deviation (MAD) was limited to 1.54 % and the average absolute deviation (AAD) was 0.38 %. Moreover, excellent agreement between measured density and literature values further confirms the reliability and accuracy of the present measurements for mixtures. A kind of endothermic hydrocarbon fuel's densities data have been experimentally obtained at temperature in the range (283 to 950) K and supercritical pressures 3.0 MPa and 4.0 MPa. From the fitted curves of the densities, the isobaric thermal expansions were calculated. There was a nonmonotony tend in the curves. In the pseudocritical region and thermochemical reaction region, the peak values of the thermal expansion appear.

■ AUTHOR INFORMATION

Corresponding Author

*E-mail: qcbi@mail.xjtu.edu.cn. Fax: +86-029-8266-5287.

Funding

This work was supported by the National Natural Science Foundation of China (Grant No. 21306147), the National Science Foundation for Postdoctoral Scientists of China (Grant No. 2013M532044), and the Fundamental Research Funds for the Central Universities.

Notes

The authors declare no competing financial interest.

■ REFERENCES

(1) Berje, J.; Schedemann, A.; Gmehling, J. Liquid densities of acetone and n-heptane and excess volumes of the binary system in a wide temperature and pressure range. *Fluid Phase Equilib.* **2011**, *300*, 110−115.

(2) Schilling, G.; Kleinrahm, R.; Wagner, W. Measurement and correlation of the (p, ρ, t) relation of liquid cyclohexane, toluene, and ethanol in the temperature range from 233.15 K to 473.15 K at pressures up to 30 MPa for use as density reference liquids. *J. Chem. Thermodyn.* **2008**, *40*, 1095−1105.

(3) Anselme, M. J.; Gude, M.; Teja, A. S. The critical temperatures and densities of the n-alkanes from pentane to octadecane. *Fluid Phase Equilib.* **1990**, *57*, 317−326.

(4) Nikitin, E. D.; Pavlov, P. A.; Skripov, P. V. Measurement of the critical properties of thermally unstable substances and mixtures by the pulse-heating method. *J. Chem. Thermodyn.* **1993**, *25*, 869−880.

(5) Nikitin, E. D.; Popov, A. P. Vapor−liquid critical properties of squalane measured by the pulse-heating technique. *Fluid Phase Equilib.* **2005**, *237*, 16−20.

(6) Hooker, H. H.; Popper, G. F. *A gamma-ray attenuation method for void fraction determinations in experimental boiling heat transfer test facilities*; University of Michagan Library: Ann Arbor, MI, 1958

(7) Chan, A. M. C.; Banerjee, S. Design aspects of gamma densitometers for void fraction measurements in small scale two-phase flows. *Nucl. Instrum. Methods Phys. Res.* **1981**, *190*, 135−148.

(8) Kumara, W. A. S.; Halvorsen, B. M.; Melaaen, M. C. Single-beam gamma densitometry measurements of oil−water flow in horizontal and slightly inclined pipes. *Int. J. Multiphase Flow* **2010**, *36*, 467−480.

(9) Abdulagatov, I. M.; Azizov, N. D. (p, ρ, t, x) and viscosity measurements of {$x_1$$n$-heptane + (1 − x_1)n-octane} mixtures at high temperatures and high pressures. *J. Chem. Thermodyn.* **2006**, *38*, 1402−1415.

(10) Quevedo-Nolasco, R.; Galicia-Luna, L. A.; Elizalde-Solis, O. Compressed liquid densities for the (n-heptane + n-decane) and (n-octane + n-decane) systems from t = (313 to 363) K. *J. Chem. Thermodyn.* **2012**, *44*, 133−147.

(11) Petrick, M. Radiation attenuation method of measuring density of a two-phase fluid. *Rev. Sci. Instrum.* **1958**, *29*, 1079.

(12) Jiang, Y. ; Rezkallah, K. S. An experimental study of the suitability of using a gamma densitometer for void fraction measurements in gas−liquid flow in a small diameter tube *Meas. Sci. Technol.* **1993**, *4*.

(13) Pecar, D.; Dolecek, V. Isothermal compressibilities and isobaric expansibilities of pentane, hexane, heptane and their binary and ternary mixtures from density measurements. *Fluid Phase Equilib.* **2003**, *211*, 109−127.

(14) Deng, H. W.; Zhang, C. B.; Xu, G. Q.; Tao, Z.; Zhang, B.; Liu, G. Z. Density measurements of endothermic hydrocarbon fuel at sub- and supercritical conditions. *J. Chem. Eng. Data* **2011**, *56*, 2980−2986.

(15) Eberle, C. S.; Leung, W. H.; Ishii, M.; Revankar, S. T. Optimization of a one-shot gamma densitometer for measuring area-averaged void fractions of gas-liquid flows in narrow pipelines. *Meas. Sci. Technol.* **1994**, *5*, 1146.

(16) Chaouki, J.; Larachi, F.; Duduković, M. P. Noninvasive tomographic and velocimetric monitoring of multiphase flows. *Ind. Eng. Chem. Res.* **1997**, *36*, 4476−4503.

(17) Stahl, P.; von Rohr, P. R. On the accuracy of void fraction measurements by single-beam gamma-densitometry for gas−liquid two-phase flows in pipes. *Exp. Therm. Fluid Sci.* **2004**, *28*, 533−544.

(18) Park, H.-S.; Chung, C.-H. Design and application of a single-beam gamma densitometer for void fraction measurement in a small diameter stainless steel pipe in a critical flow condition. *Nucl. Eng. Technol.* **2007**, *39*, 349−357.

(19) Jiang, R. P.; Liu, G. Z.; You, Z. Q.; Luo, M. J.; Wang, X. Q.; Wang, L.; Zhang, X. W. On the critical points of thermally cracked

hydrocarbon fuels under high pressure. *Ind. Eng. Chem. Res.* **2011**, *50*, 9456−9465.